# Обзор ArXiv/astro-ph 17-23 мая 2023 года

От Сильченко О.К.

# ArXiv: 2305.11219

## MUSE-ALMA Halos XI: Gas flows in the circumgalactic medium

Simon Weng,[1,2,3,4]* Céline Péroux,[1,5] Arjun Karki,[6] Ramona Augustin,[7] Varsha P. Kulkarni,[6] Aleksandra Hamanowicz,[7] Martin Zwaan,[1] Elaine M. Sadler,[2,3,4] Dylan Nelson,[8] Matthew J. Hayes,[9] Glenn G. Kacprzak,[10,3] Andrew J. Fox,[11,12] Victoria Bollo,[1] Benedetta Casavecchia,[13] Roland Szakacs,[1]

[1] *European Southern Observatory, Karl-Schwarzschildstrasse 2, D-85748 Garching bei München, Germany*
[2] *Sydney Institute for Astronomy, School of Physics A28, University of Sydney, NSW 2006, Australia*
[3] *ARC Centre of Excellence for All Sky Astrophysics in 3 Dimensions (ASTRO 3D)*
[4] *ATNF, CSIRO Space and Astronomy, PO Box 76, Epping, NSW 1710, Australia*
[5] *Aix Marseille Université, CNRS, LAM (Laboratoire d'Astrophysique de Marseille) UMR 7326, 13388, Marseille, France*
[6] *Department of Physics and Astronomy, University of South Carolina, Columbia, SC 29208, USA*
[7] *Space Telescope Science Institute, 3700 San Martin Drive, Baltimore, MD 21218, USA*
[8] *Universität Heidelberg, Zentrum für Astronomie, Institut für theoretische Astrophysik, Albert-Ueberle-Str. 2, 69120 Heidelberg, Germany*
[9] *Stockholm University, Department of Astronomy and Oskar Klein Centre for Cosmoparticle Physics, AlbaNova University Centre, SE-10691, Stockholm, S*
[10] *Centre for Astrophysics and Supercomputing, Swinburne University of Technology, Hawthorn, Victoria 3122, Australia*
[11] *AURA for ESA, Space Telescope Science Institute, 3700 San Martin Drive, Baltimore, MD 21218, USA*
[12] *Department of Physics & Astronomy, Johns Hopkins University, 3400 N. Charles St., Baltimore, MD 21218*
[13] *Max-Planck-Institut für Astrophysik, Karl-Schwarzschild-Strasse 1, D-85748 Garching b. München, Germany*

# Закончили наконец обзор!

The MUSE-ALMA Halos survey targets 32 Ly-$\alpha$ absorbers with column densities $\log[N(\mathrm{H\,I})/\mathrm{cm}^{-2}] > 18.0$ at redshift $0.2 \lesssim z \lesssim 1.4$ (see Péroux et al. 2022, for an overview). In total, 79 galaxies are detected within $\pm 500$ km s$^{-1}$ of the absorbers at impact parameters ranging from 5 to 250 kpc (Weng et al. 2022). The stellar masses of these associated galaxies have been measured from broadband imaging in Augustin et al. (in prep) and their morphologies studied in Karki et al. (submitted). Gas flows for a subsample of galaxies have already been studied in earlier works (Péroux et al. 2017; Klitsch et al. 2018; Rahmani et al. 2018a,b; Hamanowicz et al. 2020; Szakacs et al. 2021) and our work is a continuation of these studies for the full MUSE-ALMA Halos survey. With the complete sample of absorbers and their galaxy counterparts, we examine the azimuthal dependence of metallicity in the circumgalactic medium and identify the gas flows being probed by QSO sightlines. We adopt the following $\Lambda$CDM cosmology: $H_0 = 70$ km s$^{-1}$ Mpc$^{-1}$, $\Omega_M = 0.3$ and $\Omega_\Lambda = 0.7$.

**Table 2. Sample summary of modelled galaxies.** We consider only the sample of modelled galaxies with inclinations $i > 30°$ to limit potential errors in the position angle measurement.

| Criterion | Tool | Number | **Total** |
|---|---|---|---|
| Kinematic modelling | GALPAK | 48 | |
| Photometric modelling | GALFIT | 19 | **79** |
| Not modelled | | 12 | |
| Inclination $> 30°$ | | 56 | **67** |
| Inclination $< 30°$ | | 11 | |

**Статистика плавает:**
**27 систем линий поглощения водорода,**
**48 галактик с полем скоростей MUSE**

# Сравнение скорости линии поглощения водорода с полем скоростей ионизованного газа

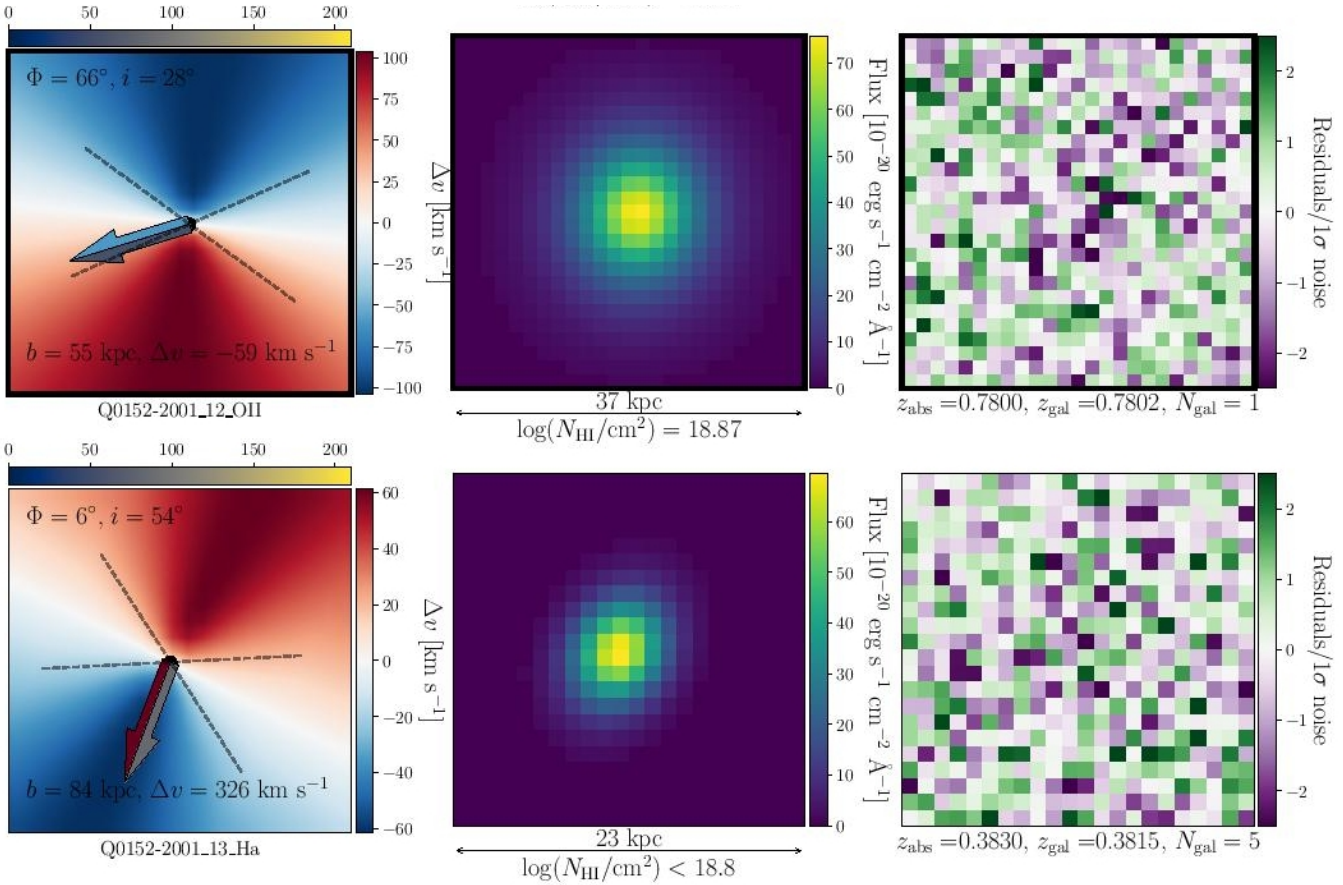


**Figure 1.** The modelled velocity, observed flux and residual maps of three randomly chosen galaxies associated with QSO absorbers that were fitted using

# Статистика: угол от большой (кин.) оси – прицельный параметр

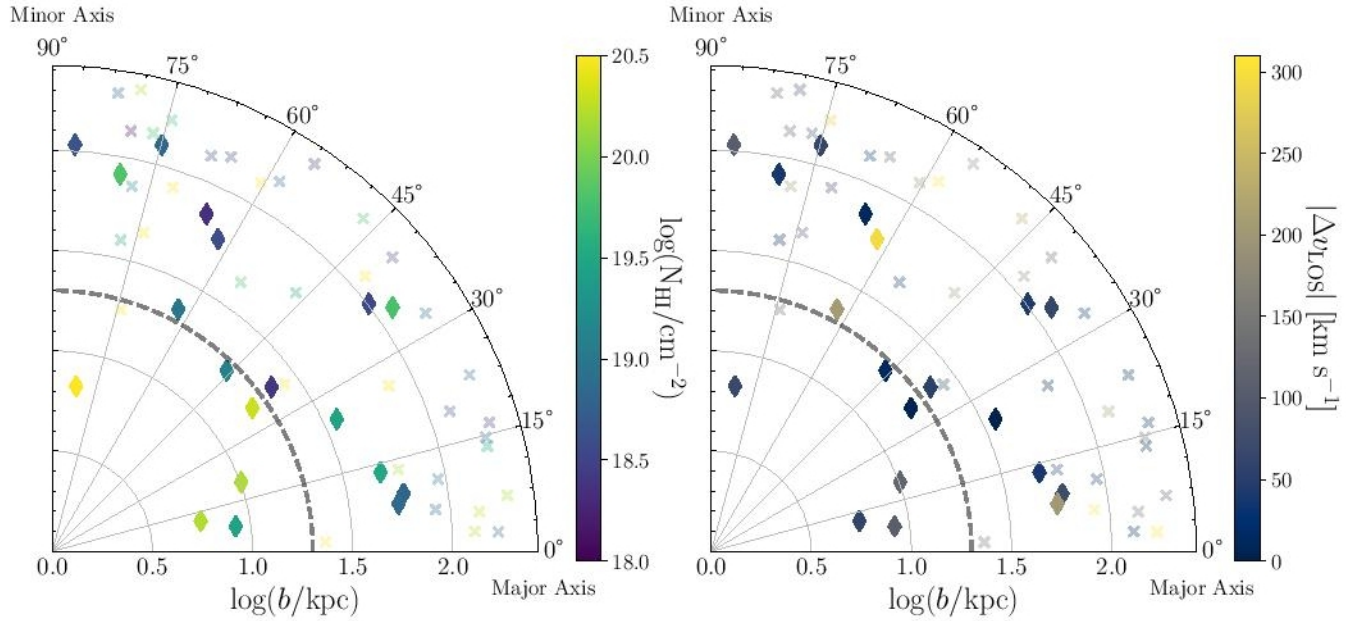


**Figure 3.** Polar plots illustrating the distribution of the H I absorbers as a function of azimuthal angle and impact parameter. Diamonds represent galaxies that are found at closest impact parameter to a given absorber and each point is coloured by the H I column density (left) or the absolute value of the line of sight velocity difference between galaxy and absorber (right). Crosses show the location of associated galaxies at larger impact parameters when multiple galaxies are associated with a single absorber. Points located near 90° are found near the galaxy minor axis. The black dashed line marks an impact parameter of $b = 20$ kpc.

# Бимодальность по углу?

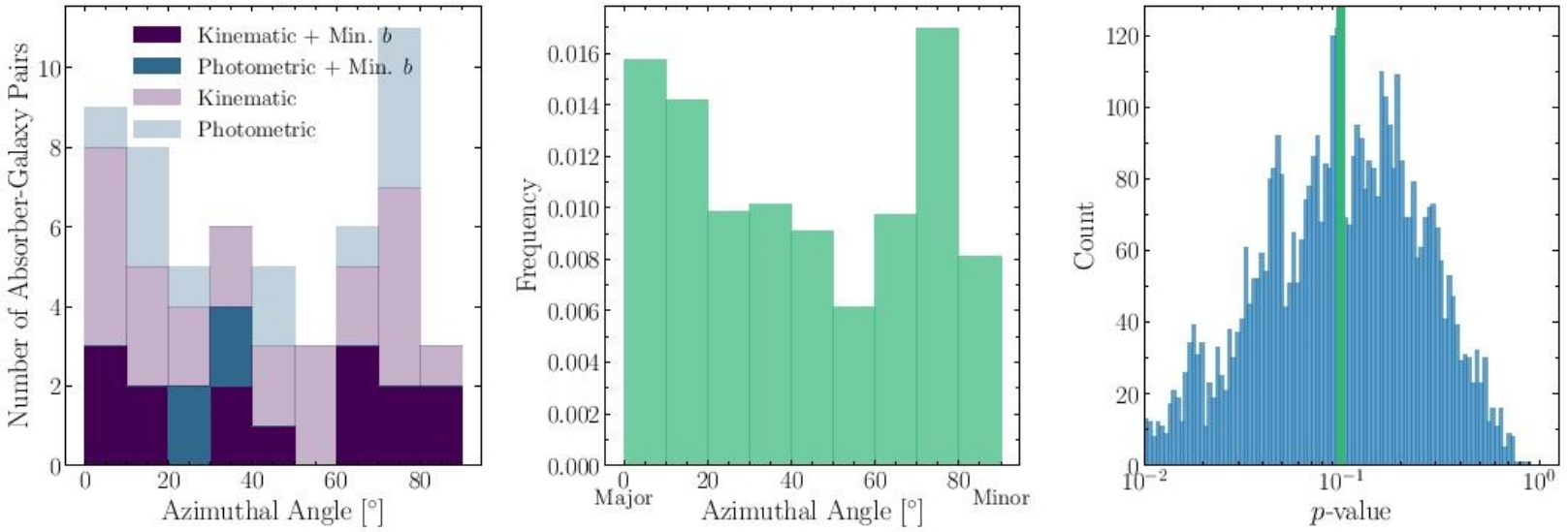


**Figure 2.** The distribution of azimuthal angles between absorbers and galaxies with inclination $i > 30°$. We set this restriction on the inclination to remove face-on galaxies with large errors in their modelled position angle. In the left histogram, the purple and blue colours respectively represent galaxies with measured kinematic and photometric PAs, derived from modelling the MUSE cubes and HST imaging respectively. Opaque bars represent galaxies found at the closest impact parameter to the QSO sightline, while translucent bars represent PA measurements of the other galaxy counterparts further from the absorber. To test whether the distribution of azimuthal angles is bimodal, we generate 5,000 iterations of the initial distribution by randomly sampling the uncertainties in $\Phi$ and perform the Hartigan's dip test for each iteration (Hartigan & Hartigan 1985). The final frequency distribution from the 5,000 samples is shown in the middle histogram and the corresponding distribution of $p$-values are shown on the right. The median $p$-value is $\approx 0.1$ (indicated by the vertical green bar) which suggests there is marginal evidence for a bimodal distribution in azimuthal angles.

# Корреляция металличности линий в спектре квазара с углом?

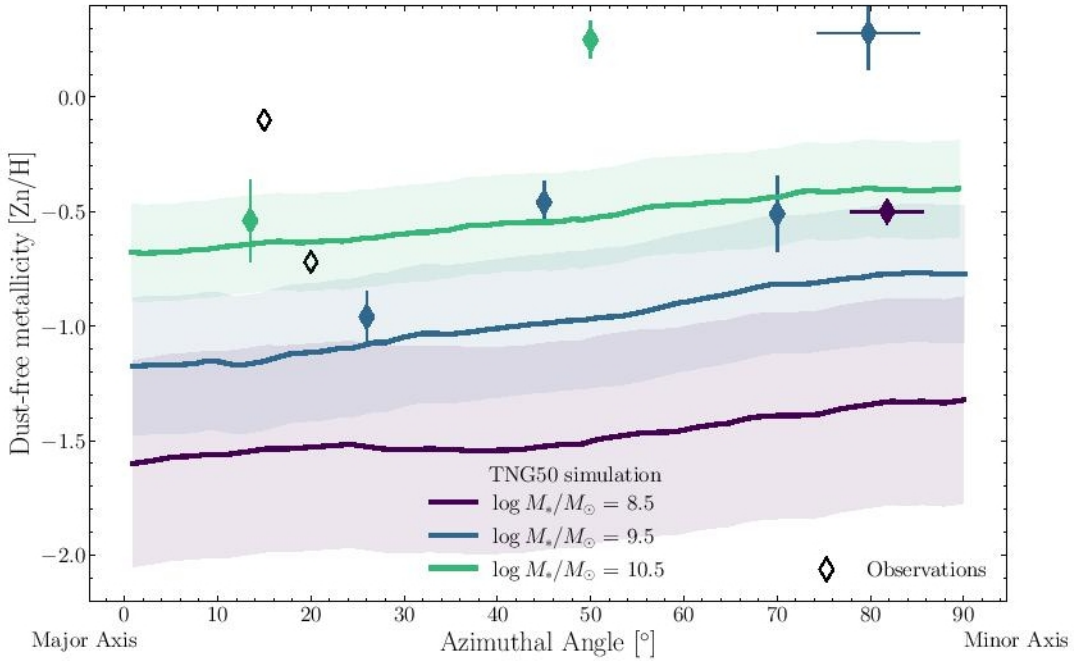


**Figure 4.** The absorber metallicity as a function of azimuthal angle. Diamonds represent results from this survey and previous works (Péroux et al. 2011, 201 Bouché et al. 2013, 2016) that measured metal abundances directly. The coloured lines are the trends predicted by the TNG50 simulation (Péroux et al. 202 for galaxies of different stellar masses at $z = 0.5$ and $b = 100$ kpc. The shaded regions represent a $1\sigma$ deviation. Each galaxy is coloured by their stellar ma corresponding to the coloured lines, while the unfilled black diamonds are galaxies without $M_*$ measurements. At present, there are too few H I absorbers wi robust metallicities and galaxy counterparts to confirm gas near the minor axis is more metal-enriched than gas near $\Phi = 0°$.

# Каждая из 27 систем отклассифицирована

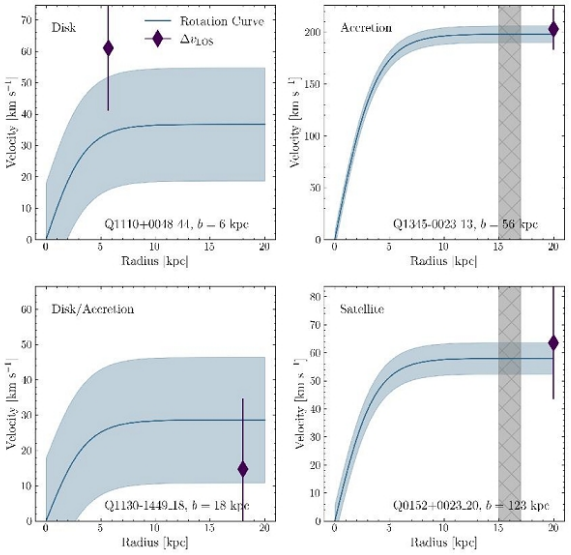


**Figure 5.** Comparisons between the galaxy rotation curve and absorber line of sight velocities for cases where the disk or gas accretion is being traced. The blue line represents the galaxy rotation curve modelled by a hyperbolic tangent and the shaded region represent the $1\sigma$ error. We plot the velocity of the absorber relative to the systemic redshift of the galaxy as a purple diamond. A vertical hatched region is used to illustrate that the impact parameter of the absorber is beyond the limits of the $x$-axis. We provide the gas flow origin in text at the top-left, while the galaxy ID and absorber impact parameter are found at the bottom of each plot. In three cases, we find the absorber velocity is consistent with the rotating disk or co-rotating halo of the galaxy at nearest impact parameter. For the bottom-right case, the absorber is beyond the virial radius of the nearest galaxy and likely arises from a faint, quiescent galaxy.

- Индивидуальная классификация:

- Log(N(HI))>20.2, b<20 kpc, участвует во вращении – собственный диск
- Угол <30 градусов, участвует во вращении, log(N(HI))<19 – аккреция
- Угол >60 градусов, НЕ участвует во вращении - ветер

# Результаты

- 1(+3) – диск
- 3 – аккреция
- 3(+4?) – ветер
- Из 27… остальное, вероятно, – множественные системы на луче зрения, невидимые карлики, внутригрупповая среда.

# Характеристики ветра

**Table 3. Comparison of line of sight absorber velocity with the escape velocity for galaxy-absorber pairs consistent with outflows.** The line of sight velocity of the absorber relative to the galaxy is roughly equal to the escape velocity assuming a singular isothermal sphere. Given that $\Delta v_{\rm LOS}$ does not account for velocities orthogonal to the line of sight, it is possible that the H I absorbers trace neutral gas escaping the potential of the galaxy. While $|\Delta v_{\rm LOS}| < V_{\rm esc}$, the radial velocity of the gas may be larger than the escape velocity.

| QSO | $z_{\rm abs}$ | $\log N$ (H I) $\log({\rm cm}^{-2})$ | $b$ kpc | $\lvert\Delta v_{\rm LOS}\rvert$ km s$^{-1}$ | $V_{\rm esc}$ km s$^{-1}$ |
|---|---|---|---|---|---|
| Q0454+039 | 1.1532 | 18.59 | 60 | 290 | 300 |
| Q1229−021 | 0.3950 | 20.75 | 6 | 70 | 80 |
| Q1554−203 | 0.7869 | <19.0 | 23 | 210 | 270 |

*4.3.1 Does the gas escape?*

We can determine whether the neutral gas escapes the galaxy halo by comparing the absorber velocity with the escape velocity ($V_{\rm esc}$). The escape velocity at a given radius, $r$, is calculated assuming a singular isothermal sphere (Veilleux et al. 2005):

$$V_{\rm esc} = V_{\rm vir} \times \sqrt{2\left(1 + \ln \frac{R_{\rm vir}}{r}\right)}, \quad (1)$$

where $V_{\rm vir}$ and $R_{\rm vir}$ are the virial velocity and radius respectively. Here, we assume the radius to be the impact parameter ($r \approx b$). We estimate $V_{\rm vir}$ using the prescription in Schroetter et al. (2019) where $V_{\rm vir} \approx 1.2 \times S_{0.5}$. Here, $S_{0.5} = \sqrt{0.5 \times V_{\rm max}^2 + \sigma^2}$ is the kinematic estimator and is a function of the rotational velocity and velocity dispersion, $\sigma$ (Weiner et al. 2006). Using $V_{\rm vir}$, we can then approximate the virial radius to be $R_{\rm vir} \approx V_{\rm vir}/10H(z)$ where $H(z)$ is the Hubble constant at redshift $z$. The estimated escape velocity values are tabulated in Table 3.

# Поиски корреляций с характеристиками галактик

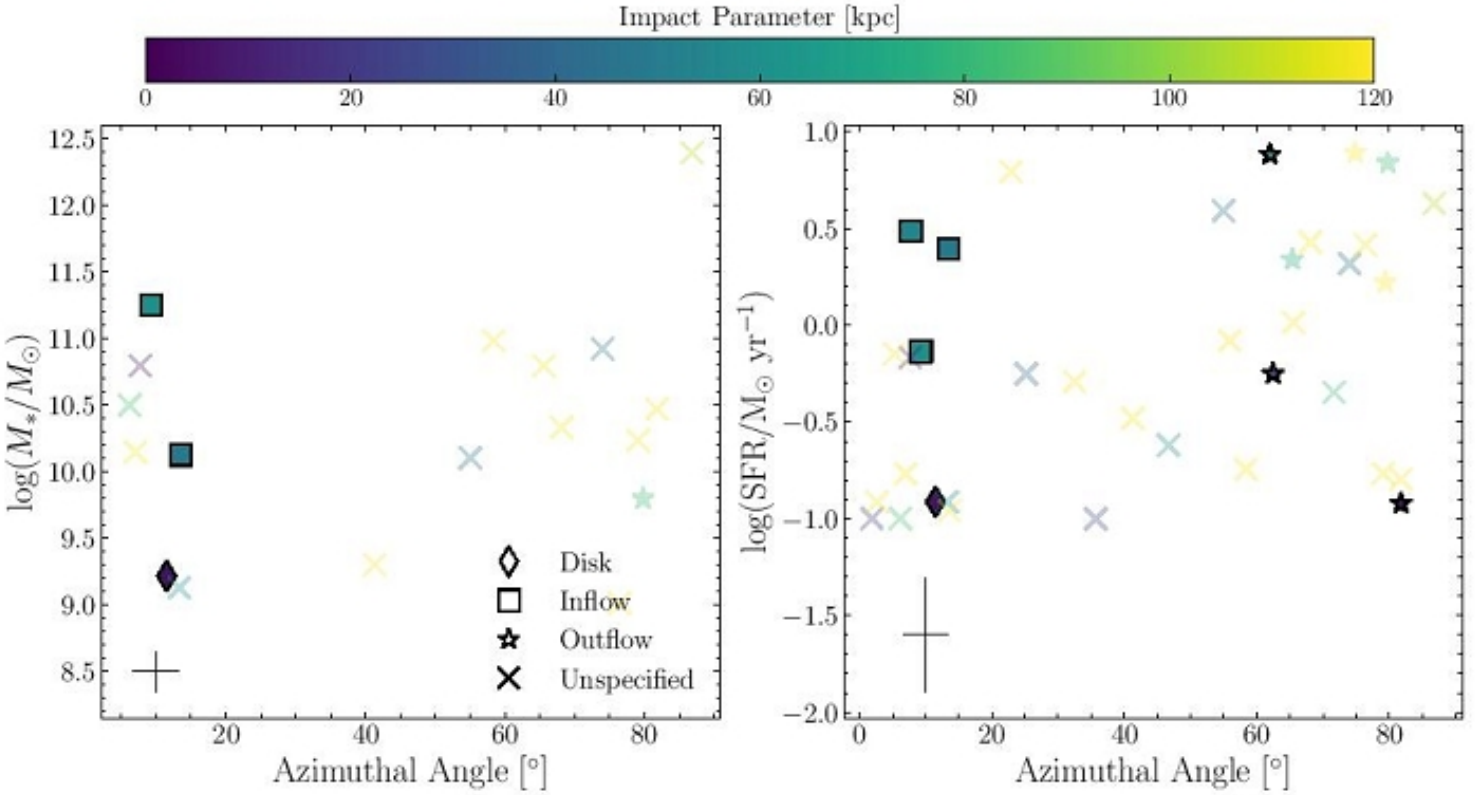


**Figure 6.** The stellar properties of the galaxies associated with an absorber. The left plot shows the stellar mass of galaxies associated with absorbers at a given azimuthal angle. Stellar masses are derived from spectral energy distribution (SED) fitting of the HST broadband imaging (Augustin et al. in prep). Different symbols represent galaxy-absorber pairs that are found to trace inflowing, outflowing or gas in the disk while faint crosses represent pairs with ambiguous origins. Symbols with a black border are cases where the gas origin has been confidently identified, while those with lower transparency are possible cases. Each galaxy is coloured by the impact parameter from the absorber. We find absorbers are associated with galaxies that span four dex in stellar mass. On the right, we show the dust-uncorrected star-formation rate of galaxies measured using the H$\alpha$ or [O II] emission lines (Weng et al. 2022). We find that the galaxies associated with inflows and outflows do not differ significantly in their SFRs. The median errors in the plotted properties are shown as a cross in the bottom left of both plots.